AJNR

Differentiation Between Classic and Atypical Meningiomas with Use of Diffusion Tensor Imaging

C.-H. Toh, M. Castillo, A.M.-C. Wong, K.-C. Wei, H.-F. Wong, S.-H. Ng and Y.-L. Wan

AJNR Am J Neuroradiol 2008, 29 (9) 1630-1635
doi: https://doi.org/10.3174/ajnr.A1170
http://www.ajnr.org/content/29/9/1630

ORIGINAL RESEARCH

Differentiation Between Classic and Atypical Meningiomas with Use of Diffusion Tensor Imaging

C.-H. Toh
M. Castillo
A.M.-C. Wong
K.-C. Wei
H.-F. Wong
S.-H. Ng
Y.-L. Wan

BACKGROUND AND PURPOSE: The differentiation between classic and atypical meningiomas may have implications in preoperative planning but may not be possible on the basis of conventional MR imaging. Our hypothesis was that classic and atypical meningiomas have different patterns of intratumoral water diffusion that will allow for differentiation between them.

MATERIALS AND METHODS: Preoperative diffusion tensor imaging (DTI) was performed in 12 classic and 12 atypical meningiomas. Signal intensity of solid-enhancing tumor regions on diffusion-weighted trace images and apparent diffusion coefficient (ADC) and fractional anisotropy (FA) maps was assessed. Regions of interest (ROIs) were placed in solid-enhancing regions, peritumoral edema, and contralateral normal-appearing white matter (NAWM) to measure tensor metrics including major (λ_1), intermediate (λ_2) and minor eigenvalues (λ_3) and FA and ADC values. Distribution of tensor shapes within enhancing tumors was calculated for all tumors. Differences between classic and atypical meningiomas in tumor signal intensity, intratumoral and peritumoral tensor metrics, as well as tensor shapes distribution were statistically analyzed.

RESULTS: A significantly greater proportion of atypical meningiomas were isointense and hypointense on ADC maps ($P = .007$). Classic meningiomas had significantly lower FA ($P = .012$), higher ADC ($P = .011$), greater λ_2 ($P = .020$) and λ_3 ($P = .003$). There was significantly more spherical diffusion in classic than in atypical meningiomas ($P = .020$). All diffusion tensor metrics for peritumoral edema of the 2 tumor groups did not differ.

CONCLUSION: DTI showed that intratumoral microscopic water motion is less organized in classic than in atypical meningiomas. This feature may allow for noninvasive differentiation between classic and atypical meningiomas.

Meningiomas account for between 16% and 20% of primary intracranial tumors.[1] According to the World Health Organization (WHO) classification system, 78% of meningiomas are grade I, 20.4% are grade II, and 1.6% are grade III.[2] Grades II and III meningiomas are more aggressive than grade I meningiomas. Five-year recurrence rates are 12% for benign meningiomas and 41% for atypical meningiomas.[2] Initial extent of tumor resection and histologic grade are key determinants for recurrence.[3] Therefore, prospectively identifying their histologic grades can be clinically beneficial in treatment planning. Although conventional MR imaging can provide detailed morphologic information of meningiomas, its value in the prediction of WHO grades is limited.[4]

According to the WHO classification,[5] classic meningiomas differ from atypical ones in their number of mitoses, cellularity, and nucleus-to-cytoplasm ratio (N/C ratio) as well as their histologic patterns. Complex microstructural barriers in brain tissue, such as white matter tracts, cell membranes, and capillary vessels result in a tendency for water molecules to diffuse with direction (anisotropic diffusion) rather than equally in all directions (isotropic diffusion). Isotropic diffusion-weighted imaging (DWI), which measures average magnitude of water motion in apparent diffusion coefficient (ADC), has shown controversial results for differentiating classic from atypical meningiomas.[6–8] In contrast to isotropic DWI, diffusion tensor imaging (DTI) provides information about magnitude and directionality of water diffusion[9] and thus may be able to measure the differences in intratumoral diffusion anisotropy as a result of histologic differences between classic and atypical meningiomas. On the other hand, peritumoral edema associated with meningiomas, regardless of classic or atypical subtypes, has always been considered a purely vasogenic edema (ie, absence of tumor cell infiltration).[10,11]

Our first hypothesis was that intratumoral diffusion anisotropy is different between these 2 tumor types and that differences in diffusion anisotropy as detected by DTI allow differentiation between them. Our second hypothesis was that anisotropic diffusion measured in peritumoral edema with DTI will not be different between classic and atypical meningiomas.

Materials and Methods

Patients

We obtained approval for this study from the Institutional Board of Research Associates and obtained signed informed consent from all patients. Patient identifiers were removed from image data before analysis. No patients had begun corticosteroid treatment or radiation therapy, and none had previous brain biopsy at the time of MR imaging. MR examinations were performed in 12 patients (7 men, 5

Received March 2, 2008; accepted after revision April 16.

From the Departments of Medical Imaging and Intervention (C.-H.T., A.M.-C.W., H.-F.W., S.-H.N., Y.-L.W.) and Neurosurgery (K.-C.W.), Chang Gung Memorial Hospital and Chang Gung University College of Medicine, Tao-Yuan, Taiwan; and Department of Radiology (M.C.), University of North Carolina School of Medicine, Chapel Hill, NC.

Please address correspondence to Cheng-Hong Toh, MD, Department of Medical Imaging and Intervention, Chang Gung Memorial Hospital, Chang Gung University College of Medicine, 5 Fu Hsing St, Kwei Shan Hsiang, Tao-Yuan 333, Taiwan; e-mail: eldomtoh@hotmail.com

DOI 10.3174/ajnr.A1170

women; mean age, 55.2 years; age range, 38–71 years) with classic meningiomas (WHO grade I) and 12 patients (5 men, 7 women; mean age, 56.3 years; age range, 24–80 years) with atypical meningiomas (WHO grade II). Histologic diagnosis was obtained in all patients. Subtypes of meningiomas were classified according to the WHO (2007) classification.[5] An atypical meningioma has increased mitotic activity, which is defined as 4 or more mitoses per 10 high-power fields or with 3 or more of the following features: 1) increased cellularity, 2) small cells with a high nucleus-to-cytoplasm ratio, 3) prominent nucleoli, 4) uninterrupted patternless or sheetlike growth, and 5) foci of "spontaneous" or "geographic" necrosis. Subtypes of classic meningiomas included 7 meningothelial, 2 fibroblastic, 2 transitional, and 1 psammomatous meningioma. Peritumoral edema was present in 9 (75%) of 12 patients with classic meningiomas and 8 (66.6%) of 12 patients with atypical meningiomas. Tumors with large calcifications, hemorrhages, or both were excluded.

MR Imaging

All patients underwent MR imaging including axial T2-weighted, DWI, DTI, and axial spin-echo T1-weighted imaging (T1WI) performed before and after intravenous administration of 0.1 mmol/kg body weight of gadopentetate dimeglumine (Magnevist; Schering, Berlin, Germany). All MR imaging studies were performed on a single occasion with a 3T unit (Magnetom Tim Trio; Siemens, Erlangen, Germany). DTI was performed in the axial plane with single-shot echo-planar imaging with the following parameters: TR, 8600 ms; TE, 91 ms; diffusion gradient encoding in 12 directions; $b = 0$; 1000 seconds/mm^2; FOV, 192 × 192 mm; matrix size, 128 × 128; section thickness, 3 mm; and number of signal intensity acquired, 5. A total of 35 to 40 sections were used to cover the cerebral hemispheres, upper brain stem, and cerebellum without gaps. To minimize artifacts such as signal intensity drop-out and gross geometric distortions associated with the echo-planar imaging, we used the parallel imaging technique (generalized autocalibrating partially parallel acquisitions[12] with a reduction factor of 2) during DTI acquisitions.

Image Postprocessing

We transferred diffusion tensor data to an independent workstation and processed using the software nordicICE (nordic Image Control and Evaluation Version 2.2; Nordic Imaging Lab, Bergen, Norway). The diffusion tensor was diagonalized to yield the major (λ_1), intermediate (λ_2), and minor (λ_3) eigenvalues. Voxel by voxel, the fractional anisotropy (FA), directionally averaged ADC (also known as mean diffusivity), and distribution of linear (C_l), planar (C_p), or spherical (C_S) tensor shapes[13] were calculated with the following respective standard algorithms:

$$\mathrm{ADC} = \bar{\lambda} = \frac{\lambda_1 + \lambda_2 + \lambda_3}{3},$$

$$\mathrm{FA} = \sqrt{\frac{3}{2}} \cdot \sqrt{\frac{(\lambda_1 - \bar{\lambda})^2 + (\lambda_2 - \bar{\lambda})^2 + (\lambda_3 - \bar{\lambda})^2}{\lambda_1^{\,2} + \lambda_2^{\,2} + \lambda_3^{\,2}}}$$

$$C_l = \frac{\lambda_1 - \lambda_2}{\lambda_1 + \lambda_2 + \lambda_3},$$

$$C_p = \frac{2 \cdot (\lambda_2 - \lambda_3)}{\lambda_1 + \lambda_2 + \lambda_3},$$

and

$$C_S = \frac{3\lambda_3}{\lambda_1 + \lambda_2 + \lambda_3}.$$

Imaging Analysis

Two neuroradiologists performed qualitative visual inspections of DW trace images and ADC and FA maps with consensus reading. On DW trace images and ADC maps, each lesion was categorized as being predominantly hyperintense, isointense, or hypointense relative to the cortex. On FA maps, signal intensity was judged as predominantly hypointense if similar to that of the cortex, hyperintense if similar to white matter, and otherwise as mixed signal intensity.

With use of the coregistration module integrated of nordicICE, the λ_1, λ_2, λ_3, and FA and ADC maps were automatically co-registered to postcontrast T1WI on the basis of DICOM geometry parameters. The adequacy of registration was visually assessed by the 2 observers, and manual adjustments were performed if necessary. Circular regions of interest (ROIs) with diameters ranging from 1 to 1.5 cm were placed centrally within the largest solid-enhancing area of all meningiomas and peritumoral area if edema was present (Figs 1 and 2). ROIs were then automatically transferred to the co-registered λ_1, λ_2, λ_3, and FA and ADC maps. ROIs were copied onto the corresponding contralateral normal-appearing white matter (NAWM) in each patient to obtain the λ_1, λ_2, λ_3, and FA and ADC values for the purpose of normalization. The neuroradiologist placing the ROIs was blinded to the individual diagnoses. For each ROI within the enhancing tumor, the distribution of tensor shapes—categorized as linear, planar, and spherical—was calculated.

Statistical Analysis

Differences in signal intensities on DW trace images and ADC and FA maps between classic and atypical meningiomas were compared with a χ^2 test. Mean λ_1, λ_2, λ_3, and FA and ADC values were evaluated for each ROI. The ratios of λ_1, λ_2, λ_3, and FA and ADC were calculated by dividing λ_1, λ_2, λ_3, and FA and ADC values in the solid-enhancing tumor areas or peritumoral edema, if present, by λ_1, λ_2, λ_3, and FA and ADC values of the contralateral NAWM in the same patient. Comparisons between solid-enhancing areas of classic and atypical meningiomas and corresponding contralateral NAWM were performed with use of paired t tests. Mean absolute values and ratios of λ_1, λ_2, λ_3, and FA and ADC of solid-enhancing areas and peritumoral edema, as well as the distribution of tensor shapes of the solid-enhancing areas for the 2 tumor types were compared with a 2-sample t test. A commercially available statistical software package (SPSS 15; SPSS, Chicago, Ill) was used for analysis, and P values less than .05 were considered to indicate statistically significant differences.

Results

Qualitative Visual Inspections of DW Trace Images and ADC and FA Maps

Results of qualitative comparison of DW trace images and ADC and FA maps between classic and atypical meningiomas are summarized in Table 1. There were 9 (75%) of 12 classic meningiomas that were hyperintense and 3 (25%) of 12 that were isointense or hypointense on DW trace images. All 12 atypical meningiomas were hyperintense on DW trace images. Differences in signal intensity on DW trace images between classic and atypical meningiomas were not significant (P = .064). On ADC maps, 9 of 12 classic meningiomas were hyperintense, 3 (25%) of 12 were isointense; none was hypointense. On ADC maps, 2 (16.6%) of 12 atypical meningiomas were hyperintense, 5 (41.7%) of 12 were isointense, and 5 (41.7%)

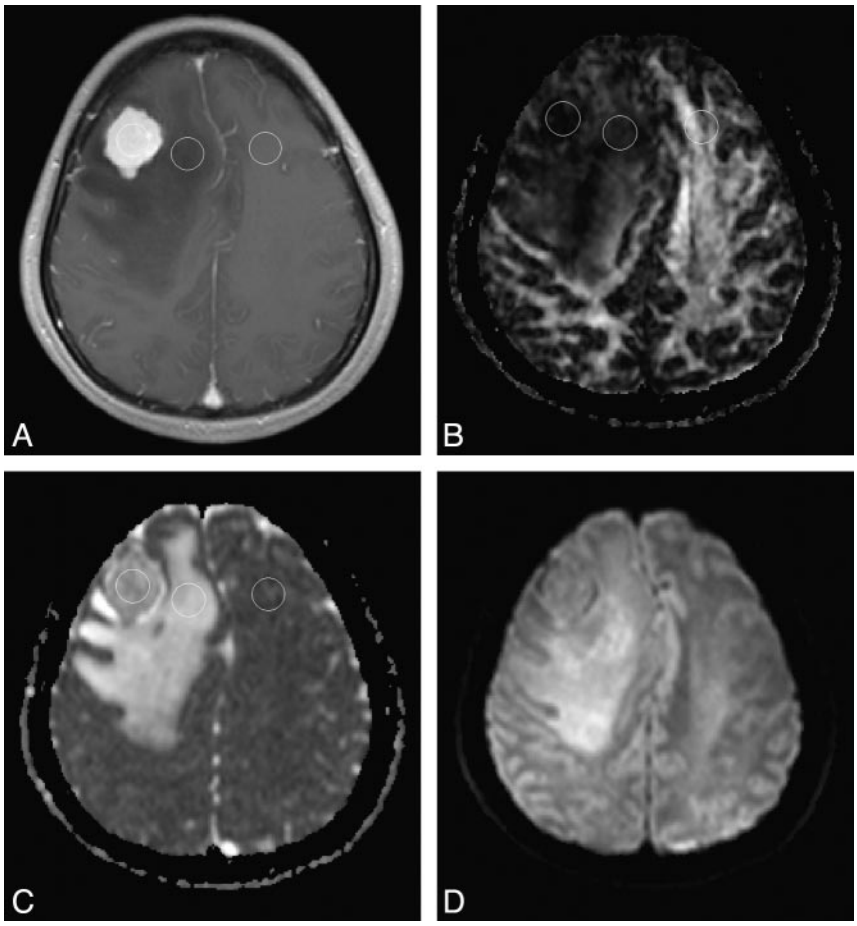

Fig 1. ADC and FA measurements in a 54-year-old woman with a pathologically confirmed classic meningioma arising in right frontal convexity. *A,* Axial contrast-enhanced T1-weighted MR image shows an enhancing mass projecting inferiorly into the right frontal lobe. Three ROIs are outlined in the enhancing tumor area, peritumoral edema, and contralateral NAWM, respectively, for measurement of λ_1, λ_2, λ_3, and ADC and FA values. FA (*B*) and ADC (*C*) maps show location of ROIs. The tumor is isointense to the cortex on axial diffusion-weighted trace image (*D*).

of 12 were hypointense. Differences in signal intensities on ADC maps between classic and atypical meningiomas were significant ($P = .007$). One (8.3%) classic meningioma was hyperintense, 8 (66.7%) of 12 had mixed signal intensity, and 3 (25%) of 12 were hypointense on FA maps. There were 3 (25%) of 12 atypical meningiomas that were hyperintense, 8 (66.7%) of 12 that had mixed signal intensities, and 1 (8.3%) of 12 that was hypointense on FA maps. Differences in signal intensities on FA maps between classic and atypical meningiomas were not significant ($P = .368$).

Mean FA Values and FA Ratios

Results of quantitative comparison intratumoral and peritumoral FA between classic and atypical meningiomas are summarized in Tables 2 and 3, respectively. Mean FA values of solid-enhancing areas of classic meningiomas and contralateral NAWM were 0.230 ± 0.085 (range, 0.085–0.365) and 0.517 ± 0.052 (range, 0.433–0.583), respectively ($P < .001$). Mean FA values of solid-enhancing areas of atypical meningiomas and contralateral NAWM were 0.336 ± 0.105 (range, 0.212–0.622) and 0.517 ± 0.061 (range, 0.427–0.612), respectively ($P < .001$). Mean FA values of solid-enhancing areas of classic meningiomas were significantly lower than those of atypical meningiomas ($P = .012$). Mean FA ratios of solid-enhancing areas were 0.45 ± 0.16 (range, 0.15–0.67) for classic meningiomas and 0.66 ± 0.19 (range, 0.37–1.02) for atypical meningiomas ($P = .008$). The peritumoral edema of classic and atypical meningiomas was not significantly different in mean FA values and ratios.

Mean ADC Values and ADC Ratios

Results of quantitative comparison of intratumoral and peritumoral ADC between classic and atypical meningiomas are summarized in Tables 2 and 3, respectively. Mean ADC values ($\times 10^{-3}$ mm^2/s) of classic meningiomas and contralateral NAWM were 0.964 ± 0.172 (range, 0.724–1.263) and 0.763 ± 0.080 (range, 0.654–0.938), respectively ($P = .002$). Mean ADC values ($\times 10^{-3}$ mm^2/s) of atypical meningiomas and contralateral NAWM were 0.791 ± 0.129 (range, 0.586–1.057) and 0.754 ± 0.075 (range, 0.643–0.868), respectively ($P = .313$). Mean ADC values of classic meningiomas were significantly greater than those of atypical meningiomas ($P = .011$). Mean ADC ratios were 1.27 ± 0.24 (range, 0.99–1.83) for classic meningiomas and 1.05 ± 0.17 (range, 0.86–1.33) for atypical meningiomas ($P = .018$). The peritumoral edema of classic and atypical meningiomas was not significantly different in mean ADC values and ratios.

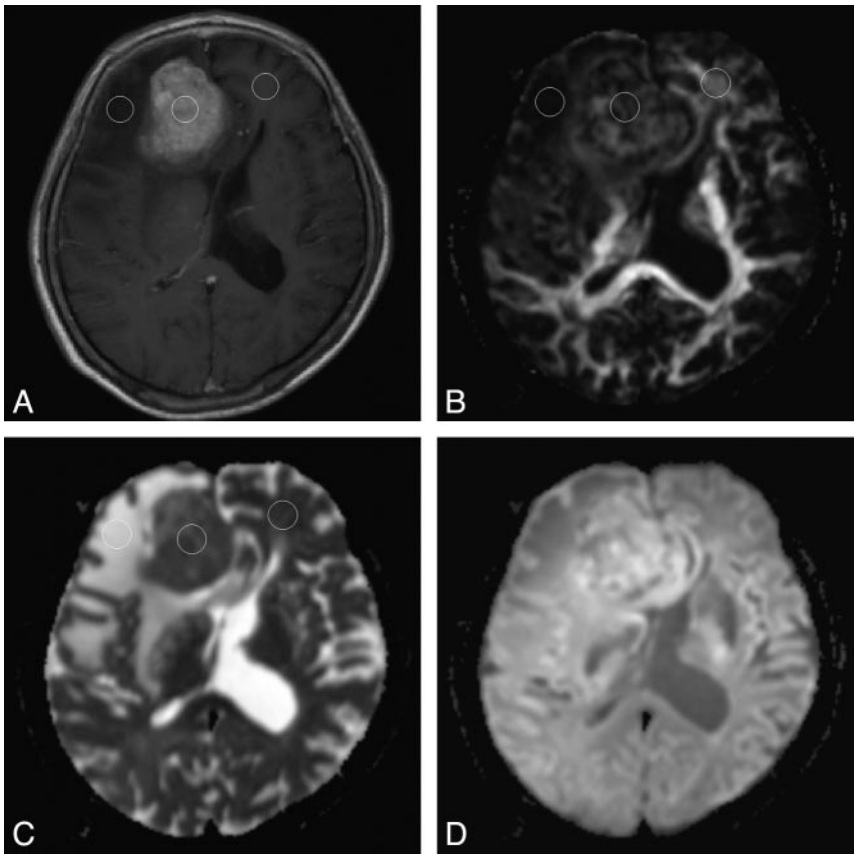

Fig 2. A 64-year-old woman with an atypical meningioma in the right frontal region confirmed on pathologic examination. Axial contrast-enhanced T1-weighted MR image (*A*) shows an enhancing mass in the right parasagittal frontal lobe. Three ROIs are outlined in the enhancing tumor area, peritumoral edema, and contralateral NAWM, respectively, for measurement of λ_1, λ_2, λ_3, and ADC and FA values. FA (*B*) and ADC (*C*) maps show location of ROIs. The tumor is hyperintense to the cortex on axial diffusion-weighted trace image (*D*).

Table 1. Tumor signal intensity assessment in classic and atypical meningiomas

Tensor Map	Classic Meningioma	Atypical Meningioma	*P* Value
ADC			.007
Hyperintense	9 (75%)	2 (16.6%)	
Isointense	3 (25%)	5 (41.7%)	
Hypointense	0 (0%)	5 (41.7%)	
DW Trace			.064
Hyperintense	9 (75%)	12 (100%)	
Isointense	3 (25%)	0 (0%)	
FA			.368
Hyperintense	1 (8.3%)	3 (25%)	
Mixed	8 (66.7%)	8 (66.7%)	
Hypointense	3 (25%)	1 (8.3%)	

Note:—FA indicates fractional anisotropy; ADC, apparent diffusion coefficient; DW, diffusion-weighted.

Mean Values and Ratios of λ_1, λ_2, λ_3

Results of quantitative comparison of intratumoral and peritumoral eigenvalues between classic and atypical meningiomas are summarized in Tables 2 and 3, respectively. Mean values ($\times 10^{-3}$ mm^2/s) of λ_1, λ_2, and λ_3 were 1.191 $\pm$ 0.202, 0.963 $\pm$ 0.183, and 0.750 $\pm$ 0.173, respectively, for classic meningiomas and 1.070 $\pm$ 0.159, 0.776 $\pm$ 0.183, and 0.541 $\pm$ 0.130, respectively, for atypical meningiomas. Mean ratios of λ_1, λ_2, and λ_3 were 0.98 $\pm$ 0.16, 1.39 $\pm$ 0.33, and 2.22 $\pm$ 0.86, respectively, for classic meningiomas and 0.89 $\pm$ 0.15, 1.15 $\pm$ 0.21, and 1.52 $\pm$ 0.61, respectively, for atypical meningiomas. Mean values and ratios of λ_2 and λ_3 of classic meningiomas were significantly greater than those of atypical meningiomas. Mean λ_1 values and ratios, on the other hand, were not significantly different between the 2 types of tumors. The peritumoral edema of classic and atypical meningiomas was not significantly different in mean λ_1, λ_2, and λ_3 values and ratios.

Tensor Shapes Assessment

Results of intratumoral tensor shape distributions in classic and atypical meningiomas are summarized in Table 4. Mean percentages of linear, planar, and spherical diffusion were 8.1% $\pm$ 3%, 14.7% $\pm$ 8%, and 77.2% $\pm$ 10%, respectively, for classic meningiomas and 13% $\pm$ 8%, 19.4% $\pm$ 8%, and 67.6% $\pm$ 9%, respectively, for atypical meningiomas. There was significantly more spherical diffusion in classic meningiomas than in atypical meningiomas ($P = .020$). The proportions of linear and planar diffusion were higher in atypical meningiomas compared with classic meningiomas, but these differences were not statistically significant.

Discussion

Our study shows that classic and atypical meningiomas cannot be differentiated on the basis of their signal intensity on DW trace images and FA maps. However, they could be differentiated with ADC maps because atypical meningiomas were generally isointense or hypointense, whereas classic meningiomas were generally hyperintense on ADC maps. On quantitative analysis, solid-enhancing areas of classic meningiomas had

Table 2. Intratumoral quantitative tensor metrics measurements in classic and atypical meningiomas

Tensor Metric	Classic Meningioma	Atypical Meningioma	*P* Value	95% CI
FA	0.230 ± 0.085	0.336 ± 0.105	.012	−.187–.025
FA ratios	0.45 ± 0.16	0.66 ± 0.19	.008	−.354–−.061
ADC	0.964 ± 0.172	0.791 ± 0.129	.011	.044–.302
ADC ratios	1.27 ± 0.24	1.05 ± 0.17	.018	.041–.393
λ_1	1.191 ± 0.202	1.070 ± 0.159	.117	−.033–.275
λ_1 ratios	0.98 ± 0.16	0.89 ± 0.15	.172	−.043–.224
λ_2	0.963 ± 0.183	0.776 ± 0.183	.020	.032–.342
λ_2 ratios	1.39 ± 0.33	1.15 ± 0.21	.045	.005–.475
λ_3	0.750 ± 0.173	0.541 ± 0.130	.003	.080–.339
λ_3 ratios	2.22 ± 0.86	1.52 ± 0.61	.033	.061–1.325

Note:—Data are the mean ± SD. Unit of λ_1, λ_2, λ_3, and ADC values is $\times 10^{-3}$ mm^2/s. Tensor metric ratios were calculated by dividing the mean values of each tensor metric in the affected hemisphere by that in the contralateral NAWM. CI indicates confidence interval; FA, fractional anisotropy; ADC, apparent diffusion coefficient.

Table 3. Peritumoral tensor metrics measurements in classic and atypical meningiomas

Tensor Metric	Classic Meningioma	Atypical Meningioma	*P* Value	95% CI
FA	0.192 ± 0.070	0.191 ± 0.037	.969	−.058–.60
FA ratios	0.39 ± 0.16	0.37 ± 0.09	.743	−.115–.158
ADC	1.674 ± 0.271	1.544 ± 0.110	.210	−.086–.348
ADC ratios	2.09 ± 0.37	1.97 ± 0.19	.423	−.192–.433
λ_1	1.988 ± 0.255	1.863 ± 0.125	.216	−.084–.334
λ_1 ratios	1.57 ± 0.29	1.47 ± 0.05	.386	−.130–.318
λ_2	1.653 ± 0.293	1.507 ± 0.129	.203	−.091–.382
λ_2 ratios	2.36 ± 0.54	2.19 ± 0.52	.512	−.377–.724
λ_3	1.382 ± 0.321	1.273 ± 0.119	.363	−.146–.364
λ_3 ratios	3.71 ± 1.82	3.50 ± 0.80	.759	−1.259–1.679

Note:—Data are the mean ± SD. Unit of λ_1, λ_2, λ_3, and ADC values is $\times 10^{-3}$ mm^2/s. Tensor metric ratios were calculated by dividing the mean values of each tensor metric in the affected hemisphere by that in the contralateral NAWM. CI indicates confidence interval; FA, fractional anisotropy; ADC, apparent diffusion coefficient.

Table 4. Intratumoral tensor shape distributions in classic and atypical meningiomas

Tensor Shape	Classic Meningioma	Atypical Meningioma	*P* Value	95% CI
Linear (%)	8.1 ± 3	13 ± 8	.067	−.103–.004
Planar (%)	14.7 ± 8	19.4 ± 8	.154	−.113–.019
Spherical (%)	77.2 ± 10	67.6 ± 9	.020	.017–.176

Note:—CI indicates confidence interval.

significantly lower FA, higher ADC, greater λ_2 and λ_3 values, and a greater proportion of spherical tensors compared with atypical meningiomas. Greater diffusivity along transverse axes (λ_2 and λ_3) of the diffusion tensor as well as a greater proportion of spherical tensors indicate that microscopic water motion is more disorganized in classic than in atypical meningiomas. On the other hand, quantitative DTI analysis of peritumoral edema of the 2 tumor groups did not differ.

On microscopic examination, classic meningiomas consist of oval or spindle-shaped neoplastic cells that form whorls, fascicles, cords, or nodules. Histologic subtypes of classic meningiomas are based on tumoral architecture and cytologic features. Among these, the meningothelial, fibrous, and transitional variants are considered the prototypical histologic patterns of classic meningiomas.[14] A single meningioma may show a combination of meningothelial, transitional, and fibrous histologic patterns. Other variants of classic meningiomas, despite having other architectural and cytologic features, are usually combined with the 3 prototypical histologic patterns.[14] We speculate that the whorls, fascicles, cords, or nodules found in classic meningiomas may serve as microscopic physical barriers and prevent water molecules from moving in a linear fashion. Consequently, microscopic water movement in classic meningiomas lacks a coherent organization throughout the tumor that results in increased λ_2 and λ_3 as well as a greater proportion of spherical tensors. In contrast to classic meningiomas, histologic features of atypical meningiomas are often described as uninterrupted patternless or sheetlike growths. Sheetlike growth pattern refers to a lack of any specific architectural pattern within the tumor. Neoplastic cells in atypical meningiomas do not form widespread whorls, fascicles, cords, or nodules as they do in classic meningiomas. Thus, we speculate that water molecules tend to move with more directionality in atypical meningiomas because of the absence of these microscopic physical barriers. This pattern is reflected as higher diffusion anisotropy and less spherical diffusion tensors in atypical meningiomas compared with classic ones.

Besides uninterrupted patternless or sheetlike growth pattern, other histologic features of atypical meningiomas on the basis of WHO criteria include 1) 4 or more mitoses per 10 high-power fields, 2) increased cellularity, 3) small cells with a high N/C ratio, 4) prominent nucleoli, and 5) foci of spontaneous necrosis.[5] Among these, cellularity and N/C ratio of tumors correlate inversely with water diffusivity.[15] In our study, the number of tumors that were isointense or hypointense was significantly greater in atypical than in classic meningiomas (83.4% vs 25%) on the basis of qualitative analysis of ADC maps. On quantitative analysis, mean ADC values and ratios were significantly lower in atypical than in classic meningiomas. These findings reflect the greater cellularity and higher N/C ratio found in atypical meningiomas. Although

results from earlier studies on whether ADC can differentiate classic from atypical meningiomas are controversial,[6-8] the results from our study show that the ADC of these 2 tumors are different. On the other hand, although all atypical meningiomas were hyperintense on DW trace images, 75% of classic meningiomas also were hyperintense. Similar to a previous study,[8] our study shows that DW trace images cannot be used to differentiate atypical meningiomas from classic meningiomas.

A previous study[8] has found no difference in ADC between peritumoral edema of classic and atypical meningiomas. In our study, quantitative measurements of both isotropic and anisotropic water diffusion demonstrated no differences between peritumoral edema of both tumor groups. Brain invasion occurs in both classic (43%) and atypical (57%) meningiomas.[16] Although peritumoral edema of meningiomas has been proposed to be related to brain invasion,[17] it can occur without brain invasion and its pathogenesis is also related to the size of the tumor, histologic subtype, vascularity, secretory activity, tumor-related venous obstruction, and expression of sex hormones and receptors.[18] Furthermore, in meningiomas with brain invasion, the invasive neoplastic cells infiltrate only the cerebral cortex and generally do not extend into white matter.[17] Histologic analysis of peritumoral brain tissue of meningiomas with light and electron microscopy has shown only extracellular fluid accumulation. The neurons and fibers were relatively well preserved.[11] Vasogenic edema found in both tumor groups likely accounted for the absence of differences on DTI. Therefore, analysis of the diffusion anisotropy of peritumoral edema for differentiation between classic and atypical meningiomas with DTI is not useful.

Limitations of our study included, first, that the effect of microscopic tumor growth patterns on water diffusion was not quantified. Therefore, we could not definitively state that differences in diffusion anisotropy between classic and atypical meningiomas were only because of differences in tumor architecture. Second, we did not compare the cellularity in classic and atypical meningiomas, and thus we could not definitively state that the ADC differences between these 2 tumors were because of differences in cellularity. Third, we did not study other less common subtypes of WHO grade I meningiomas such as angiomatous, microcystic, secretory, and metaplastic meningiomas. From a histologic standpoint, these less common meningiomas do form specific architectural patterns. Therefore, we speculate that their diffusion anisotropy would be different from atypical meningiomas that are "featureless" on microscopic examination. In a similar fashion, other WHO grade II meningiomas (ie, chordoid and clear cell meningiomas) were not encountered during our study period.

Conclusion

In our preliminary study, classic meningiomas had significantly lower intratumoral FA, higher ADC, and greater λ_2 and λ_3 as well as a greater proportion of spherical tensors compared with atypical meningiomas. These DTI findings indicate that intratumoral microscopic water motion is more disorganized in classic than in atypical meningiomas. DTI may be helpful in the differentiation between classic meningiomas and atypical meningiomas.

References

1. Bondy M, Ligon BL. **Epidemiology and etiology of intracranial meningiomas: a review**. *J Neurooncol* 1996;29:197–205
2. Willis J, Smith C, Ironside JW, et al. **The accuracy of meningioma grading: a 10-year retrospective audit**. *Neuropathol Appl Neurobiol* 2005;31:141–49
3. Modha A, Gutin PH. **Diagnosis and treatment of atypical and anaplastic meningiomas: a review**. *Neurosurgery* 2005;57:538–50
4. Demaerel P, Wilms G, Lammens M, et al. **Intracranial meningiomas: correlation between MR imaging and histology in fifty patients**. *J Comput Assist Tomogr* 1991;15:45–51
5. Perry A, Louis DN, Scheithauer BW, et al. **Meningiomas.** In: Louis DN, Ohgaki H, Wiestler OD, et al, eds. *WHO Classification of Tumours of the Central Nervous System.* Lyon: IARC Press; 2007:164–72
6. Yamasaki F, Kurisu K, Satoh K, et al. **Apparent diffusion coefficient of human brain tumors at MR imaging.** *Radiology* 2005;235:985–91
7. Filippi CG, Edgar MA, Ulu AM, et al. **Appearance of meningiomas on diffusion-weighted images: correlating diffusion constants with histopathologic findings.** *AJNR Am J Neuroradiol* 2001;22:65–72
8. Hakyemez B, Yildirim N, Gokalp G, et al. **The contribution of diffusion-weighted MR imaging to distinguishing typical from atypical meningiomas.** *Neuroradiology* 2006;48:513–20
9. Pierpaoli C, Basser PJ. **Toward a quantitative assessment of diffusion anisotropy.** *Magn Reson Med* 1996;36:893–906
10. Cha S. **Update on brain tumor imaging: from anatomy to physiology.** *AJNR Am J Neuroradiol* 2006;27:475–87
11. Vaz R, Borges N, Cruz C, et al. **Cerebral edema associated with meningiomas: the role of peritumoral brain tissue**. *J Neurooncol* 1998;36:285–91
12. Bhagat YA, Emery DJ, Naik S, et al. **Comparison of generalized autocalibrating partially parallel acquisitions and modified sensitivity encoding for diffusion tensor imaging.** *AJNR Am J Neuroradiol* 2007;28:293–98
13. Alexander AL, Hasan K, Kindlmann G, et al. **A geometric analysis of diffusion tensor measurements of the human brain**. *Magn Reson Med* 2000;44:283–91
14. Ellison D, Love S, Chimelli L, et al. **Meningiomas.** In: *Neuropathology: A Reference Text of CNS Pathology.* Edinburgh: Mosby; 2004:703–16
15. Guo AC, Cummings TJ, Dash RC, et al. **Lymphomas and high-grade astrocytomas: comparison of water diffusibility and histologic characteristics.** *Radiology* 2002;224:177–83
16. Perry A, Stafford SL, Scheithauer BW, et al. **Meningioma grading: an analysis of histologic parameters.** *Am J Surg Pathol* 1997;21:1455–65
17. Ide M, Jimbo M, Kubo O, et al. **Peritumoral brain edema associated with meningioma–histological study of the tumor margin and surrounding brain.** *Neurol Med Chir (Tokyo)* 1992;32:65–71
18. Lobato RD, Alday R, Gomez PA, et al. **Brain oedema in patients with intracranial meningioma. Correlation between clinical, radiological, and histological factors and the presence and intensity of oedema.** *Acta Neurochir (Wien)* 1996; 138:485–93